

UNITED STATES DEPARTMENT OF THE INTERIOR  
GEOLOGICAL SURVEY

Uranium-Trend Systematics for Dating Quaternary Sediments

By

John N. Rosholt

U.S. Geological Survey

Denver, CO 80225

Open-File Report 85-298

1985

This report is preliminary and has not been reviewed for conformity with U.S. Geological Survey editorial standards. Any use of trade names is for descriptive purposes only and does not imply endorsement by the USGS.

## ABSTRACT

A new concept in uranium-series dating called uranium-trend dating has been tested extensively over the past several years to determine the reliability of this technique in estimating the time of deposition of surficial deposits ranging in age from 5,000 to about 800,000 years B.P. The open system dating technique consists of determining a linear trend from analyses of three to ten samples covering various layers or soil horizons formed in a given depositional unit. In each sample an accurate determination of the concentrations of  $^{238}\text{U}$ ,  $^{234}\text{U}$ ,  $^{230}\text{Th}$ , and  $^{232}\text{Th}$  is required. Whole-rock samples are used and analyses are made on subsamples of less than 2 mm-size fraction. Isotopic concentrations are determined by alpha spectrometry utilizing radioisotope dilution techniques.

The analytical results are plotted where  $(^{238}\text{U}-^{230}\text{Th})/^{238}\text{U}$  vs.  $(^{234}\text{U}-^{238}\text{U})/^{238}\text{U}$  ideally yields a linear array in which the slope of the line of best fit changes in a systematic way with the increasing age of the deposit. The rate of change of slope is determined by the half-period of uranium flux,  $F(0)$ , in the local environment. The flux consists of a mobile component of uranium that migrates either in solution or on colloids that through time slowly works its way through void spaces between mineral grains and produces a time-dependent trail of the daughter products,  $^{234}\text{U}$  and  $^{230}\text{Th}$ . An empirical model is based on the distribution of the trail of daughter products in the sediment, and the model compensates for changes in  $F(0)$  in response to different lithologies, textures, and climatic regimes. Analyses of units with known ages of deposition are required for time calibration of the empirical model; calibrations at 5,000 years, 12,000 years, 150,000 years, 600,000 years and 730,000 years were provided by correlations with deposits dated by radiocarbon and K-Ar.

At best, the uranium-trend ages have a potential estimated accuracy of about  $\pm 10$  percent for deposits older than 100,000 years; however, the uncertainty in the slope is strongly dependent on the quality of the linear trend regarding scatter of data points and the length of the slope line. Percentage errors in the ages are not symmetric throughout the range; they are greater both for young ( $<60,000$  years) and old ( $>600,000$  years) deposits.

Quaternary deposits from a variety of climatic and depositional environments were analyzed in this investigation. These deposits include alluvium, colluvium, eolian sand, till, loess, zeolitized volcanic ash, and

coastal marine sediments. Most of the deposits have been modified by pedogenic processes. Depending on local climatic conditions and lithologic compositions, these soils range from aridosols to spodosols. Some of the soils are buried such as coastal marine terrace paleosols. Owing to the need to explain the methodology and the results of U-trend dating as well as the influence of various geomorphic, climatic, and lithologic factors in various study areas, this report is divided into several chapters. These include an introductory chapter on the methodology of U-trend dating followed by separate chapters with different co-authors that describe the results for (a) time calibration units and deposits in the Rocky Mountain region, (b) alluvial deposits in the San Joaquin and Sacramento Valleys of California, (c) deposits in the Rio Grande and Pecos Valleys of New Mexico, (d) Quaternary deposits on the Nevada Test Site area of Nevada and California, (e) effects of fault disturbance on uranium-trend dating of calcareous alluvium on the Nevada Test Site, (f) marine deposits on the southeastern Atlantic Coastal Plain and (g) marine terrace deposits from southern California and Barbados, West Indies.

## INTRODUCTION

Extensive studies during the past three decades regarding the behavior of  $^{238}\text{U}$  and its decay products in the geologic environment have shown that radioactive disequilibrium in the  $^{238}\text{U}$  decay series is a common phenomenon. Previous work (Rosholt and others, 1966) indicated useful patterns of distribution of daughter products in soils, and further study could determine whether these patterns in host sediments define the magnitude and history of migration of uranium and its daughter products. Interpretation of abundance ratios of daughter products,  $^{234}\text{U}$  and  $^{230}\text{Th}$ , to parent  $^{238}\text{U}$  in natural systems requires an extensive knowledge of the physical and chemical behavior of the daughter products and the parent in regimes influenced by the hydrologic environment. Significant fractionation exists between  $^{234}\text{U}$  and  $^{238}\text{U}$  in nearly all of these regimes (Szabo, 1969; Ivanovich and Harmon, 1982).

Results of other studies of uranium-series disequilibrium show that uranium commonly exhibits an open-system behavior (Rosholt, 1980a). Ideally a closed system could exist throughout the history of a deposit if there has been no postdepositional migration of  $^{238}\text{U}$  or its in situ produced daughter products,  $^{234}\text{U}$  and  $^{230}\text{Th}$ ; however, open-system conditions are more common and

impose no restrictions on postdepositional migration of these radioisotopes in and out of sedimentary units. The geochemical environment during and after deposition of alluvial, colluvial, eolian, glacial, lacustrine, or marine sediments implies that distribution of associated uranium-series members must have been controlled by open-system behavior. The large number of geochemical variables in an open system precludes the definition of a rigorous mathematical model to describe uranium migration, however, an empirical approach can be used to define the parameters that reasonably explain the patterns of isotopic distribution. This approach requires independent time calibration and evaluation of the stratigraphic relationships of the deposits. Several samples from each deposit must be analyzed to define the slope of a line reflecting the isotopic distribution. In some units there are only small isotopic variations between samples, and a larger number of samples are required to define a linear trend more precisely. Study of alluvial and glacial units was stressed in development of the model because of the availability of units with age control and the importance of these units to geologic investigations.

#### Previous Work

Radioactive disequilibrium studies of the  $^{238}\text{U}$ - $^{234}\text{U}$ - $^{230}\text{Th}$  system in soil samples have been used to study the migration of uranium and thorium as a result of rock weathering (Hansen and Stout, 1968) and redeposition of transported parent material (Rosholt and others, 1966). Hansen (1965) used this isotopic system to develop a model for estimating the age of soil development in San Joaquin Valley and Sierra Nevada, California. Gamma-ray spectrometry, of both  $^{238}\text{U}$  and  $^{235}\text{U}$  decay series members, was used to estimate the weathering age of soils developed from weathered granite (Megumi, 1979). Determination of  $^{226}\text{Ra}$ , as an indicator of parent  $^{230}\text{Th}$ , and determination of  $^{232}\text{Th}$  in soil profiles, both by gamma ray spectrometry, have been used by Hansen and Huntington (1969) to trace thorium movement in soils on moraines. More recently Ku and others (1979) used  $^{230}\text{Th}/^{234}\text{U}$  data from several samples to date pedogenic carbonates by analysis of caliche rind coating pebbles in the alluvium to estimate the minimum age of deposition. Rate of formation of desert varnish has been investigated (Knauss and Ku, 1980) by uranium-series dating to establish its potential in archaeologic and geomorphologic applications. A preliminary description of U-trend dating using the model presented here was reported by Rosholt (1980b).

## Acknowledgments

The author is grateful to W. C. Carr, T. M. Cronin, J. W. Harden, J. W. Hawley, D. L. Hoover, G. M. Huestis, M. N. Machette, D. L. Marchand, L. McCarten, D. R. Muhs, J. P. Owens, K. L. Pierce, G. M. Richmond, R. R. Shroba, and W. C. Swadley for providing suggestions and samples from the many different areas covered in this investigation. A. J. Gude kindly provided samples from Lake Tecopa, and G. R. Scott and B. J. Szabo provided help in locating and sampling alluvial units in the Golden fault zone. J. R. Dooley, Jr., A. J. Bartel and C. R. McKinney helped with chemical separations on some of the glacial deposit samples from the Colorado, Wyoming, and northern Yellowstone National Park areas. C. A. Bush provided valuable help in operating the alpha spectrometers and programming the data acquisition system. K. R. Ludwig developed a computer program to obtain a York fit and automatic plot of the data.

## Purpose and Goals

The purpose of this investigation was to develop a model to describe that part of uranium migration whose end product was a predictable change of uranium and thorium isotopic ratios with time. The model was applied to deposits of known or inferred age. These deposits provide both the needed time calibration for the model as well as a basis for evaluating its reliability. If sufficient reliability can be demonstrated, an empirical radiometric dating technique, extending from a few thousand to almost a million years, would be available to aid in geologic investigation of surficial deposits.

For uranium-series dating, it would be useful to have a technique capable of dating the time of deposition of surficial deposits, rather than having to find fossil material suitable for dating by conventional closed-system uranium-series methods. The uranium-trend technique should date inception of migration of fluids through the deposit. Also, it would be useful to have a technique to estimate rates of formation of geochemical replacement deposits such as caliche, spring deposits, and dissolution residues.

If sufficient reliability can be demonstrated, this dating technique can be applied to some important geologic problems: (1) establishing fault chronologies and age of last movement, (2) rates of seismotectonic processes, (3) correlation of the marine record with that of deposits in the continental

interior, (4) correlation of continental deposits in differing climatic regimes, and (5) rates of accumulation of geochemical replacement deposits such as calcium carbonate or gypsum.

#### THEORY

The very long-lived  $^{238}\text{U}$  isotope (half life of  $4.5 \times 10^9$  years), upon radioactive decay, produces long-lived daughter products,  $^{234}\text{U}$  and  $^{230}\text{Th}$ . The half-life of  $^{234}\text{U}$  is 248,000 years; this isotope has potential as a geochemical tracer extending to about 900,000 years in the geologic past. The half-life of  $^{230}\text{Th}$  is 75,200 years and, because of its daughter-parent relation to  $^{234}\text{U}$ , it is a key isotope in nearly all uranium-series dating models (Ku, 1976). After deposition of sediments and geochemical precipitates, these deposits are subject to interactions with materials carried in waters that move through the deposits. Waters that permeate deposits contain at least small amounts of uranium; this uranium decays, producing some radioactive daughter products that are readily adsorbed on solid matrix material. In a sediment, these waters produce a unique trail of  $^{234}\text{U}$  and  $^{230}\text{Th}$  daughters that are related to each other in production and radioactive decay. If this trail of daughter products is of sufficient intensity to provide a measureable radioisotopic component in addition to the original radioisotopic content of the matrix material in the sediment, an empirical model for uranium-trend dating can be constructed. Analyses of several samples from a single deposit, each of which has slightly different physical properties and slightly different chemical compositions, are required to establish a trend line that defines the maturity of the daughter-product trail. A relatively large number of alluvial, eolian, glacial, and other types of deposits, which include several samples per unit, must be analyzed to provide the data base upon which the model is constructed.

In the geologic environment, uranium occurs chiefly in two different major phases: (1) as a resistate or fixed phase (solids dominated) where uranium is structurally incorporated in the matrix minerals, and (2) as a mobile phase (water dominated) which includes the uranium flux that migrates through a sedimentary deposit. This mobile-phase uranium is responsible for an isotopic fractionation process in the  $^{238}\text{U}$ - $^{230}\text{Th}$  series, represented by the trail of  $^{234}\text{U}$  and  $^{230}\text{Th}$  daughter products, that enables the uranium-trend dating technique to work. Another fractionation process is preferential  $^{234}\text{U}$

leaching from the fixed phase. Many of the deposits analyzed in this study are slightly moist and typically are not wet or saturated. Nevertheless, there is uranium migrating, perhaps seasonally, either in solution or on colloids, that slowly move through void spaces between mineral grains. In arid and semiarid environments, much of the mobile-phase uranium that leaves its trail of daughter products in a deposit (daughter emplacement) actually spends most of its time on the surface of dry solid grains, and only a small amount of the time in solution or suspension in actual water flow through a deposit. As a deposit undergoes interstratal alteration, some uranium isotopes are released from the fixed phase and enter the mobile phase; this process results in another form of isotopic fractionation ( $^{234}\text{U}$  displacement).

For surficial deposits, the starting point for the uranium-trend clock is the initiation of movement of water through the sediment rather than of initiation of soil development, although both of these processes may start at essentially the same time. The system equilibrium in the parent material is disturbed during and before transport, and the process of attainment of a new, readjusted, system equilibrium starts at the time of deposition. An assumption required for the model refers to the relative isotopic composition of uranium in the parent material at the time of deposition. This assumption is that sufficient mixing occurred during transport and deposition to have produced nearly the same original  $^{234}\text{U}/^{238}\text{U}$  ratio in each layer of the sediment that was included in the trend line. Divergence of the  $^{230}\text{Th}/^{238}\text{U}$  ratio from uniformity at the time of deposition would not affect the development of the uranium-trend line because such divergence, coupled with uniform  $^{234}\text{U}/^{238}\text{U}$  ratios in the sediment initially would define a line with a slope of zero. Figure 1 illustrates hypothetical isotopic development over time in a sediment using samples taken at three depths (a, b, and c).

The empirical model incorporates a component called uranium flux,  $F(0)$ . The actual physical significance of  $F(0)$  is not well understood; however, the flux varies exponentially with time in a deposit but the half period of  $F(0)$  is represented by a constant for a discrete depositional unit. It is related to the migration of mobile-phase uranium through a deposit; isotopic data for deposits of known age indicate that migration decreases exponentially with time. The following is an oversimplified example of the uranium flux in alluvium. At the time of deposition, large volumes of water pass through the

alluvium. However, after compaction and during subsequent soil development, the volumes of water passing through the alluvium are reduced significantly. It is assumed that cyclical variations of the flux caused by climatic changes can be approximated by an average flux. Both the quantity of water passing through and affecting a deposit, and the concentration of uranium in this water are components of the flux; the magnitude of the flux is a function of the concentration of uranium in the mobile phase relative to the concentration of uranium in the fixed phase. Best results should come from materials initially low in uranium content as the uranium-trend signal will override the signal from structural uranium.

The same model may be used to describe uranium-trend isotopic variations with time in some geochemical replacement deposits such as caliche and spring deposits. Prior to alteration of older host material, it is likely that radioactive equilibrium conditions existed. Geochemical replacement in the host would cause disruption of radioactive equilibrium. Analysis of dissolution residues or material that contains a significant quantity of replacement minerals sometimes are amenable to dating by the uranium-trend method (Szabo and others, 1980).

#### Uranium and Thorium Isotopic Fractionation

Studies of the long-lived isotopes in the  $^{238}\text{U}$  decay series in near-surface sediments (Rosholt and others, 1966) and in deeply buried granite (Stuckless and Ferreira, 1976; Rosholt, 1983) suggest an important mechanism that may be useful in characterizing the degree of isotopic fractionation and length of time during which uranium was mobilized in permeable zones. As dissolved  $^{238}\text{U}$  and  $^{234}\text{U}$  atoms decay by alpha disintegration, recoiling daughter nuclides of  $^{234}\text{Th}$ ,  $^{234}\text{Pa}$ ,  $^{234}\text{U}$ , and  $^{230}\text{Th}$  are adsorbed or driven into particulate matter at the solid/liquid interface. After sufficient time, this mechanism (daughter emplacement) results in solids that have  $^{234}\text{U}/^{238}\text{U}$  and  $^{230}\text{Th}/^{238}\text{U}$  activity ratios significantly higher than the equilibrium ratio of unity. A counter mechanism ( $^{234}\text{U}$  displacement) exists by which  $^{234}\text{U}$  produced by decay of structurally incorporated  $^{238}\text{U}$  is selectively displaced from mineral surfaces as a leached or alpha-recoiled decay product. The  $^{234}\text{U}$ -displacement mechanism has been extensively documented in natural samples (Osmond and Cowart, 1976), and laboratory investigations of the effects of recoiling alpha-emitting nuclei have been reported (Fleischer and Raabe,

1978). Kigoshi (1971) has shown that the concentration of  $^{234}\text{Th}$ , produced from alpha decay of  $^{238}\text{U}$  contained in fine-grained zircon crystals, increased with time in solutions in which the zircon crystals were dispersed. Fleischer (1980) reported on experiments which indicate that, in addition to the direct recoil ejection into the liquid interface, a second mechanism of  $^{234}\text{U}$  displacement results when many of the recoiling nuclei which are ejected from mineral grains become imbedded in adjacent grains and produce alpha-recoil tracks. Subsequent track etching by natural solutions releases some of the recoiled nuclei; the recoiling nuclei accompanying alpha decay have ranges of about 200A (0.02 microns) in water (Fleischer, 1983).

In contrast to  $^{234}\text{U}$  displacement, little attention has been given to the counter process which involves preferential gain of  $^{234}\text{U}$  relative to  $^{238}\text{U}$  on particulate matter (daughter emplacement). The gain results from recoiling nuclei that are ejected from solution, or from adsorbed  $^{238}\text{U}$  on surfaces at the water-particle interface, and are imbedded in adjacent grains. In this report, most of the samples of alluvium units described that are in semiarid or arid environments have an excess of  $^{234}\text{U}$  relative to  $^{238}\text{U}$ . This isotopic anomaly is most noticeable in altered 0.6 to 2 m.y. old volcanic ashes and tuffs in an arid environment at Lake Tecopa, California. Zeolites formed during early alteration show pronounced effects of  $^{234}\text{U}$  emplacement which probably are enhanced by the large surface area of this mineral. Zeolites formed during alteration of 10 m.y. old tuffs of Keg Mountain, Utah, however, are 50-percent deficient in  $^{234}\text{U}$  relative to  $^{238}\text{U}$  (Zielinski and others, 1980). These results suggest that, given sufficient time,  $^{234}\text{U}$  displacement mechanisms become predominant over  $^{234}\text{U}$  emplacement mechanisms. In this example, mechanisms of recoiling alpha-emitting nuclei and of release by natural etching of recoil tracks are so effective that one-half of all the  $^{234}\text{U}$  atoms produced by alpha decay of  $^{238}\text{U}$  structurally incorporated in zeolites were released from these minerals (Rosholt, 1980a).

Interpretation of radioactive disequilibrium in zeolitized glass at Lake Tecopa and Keg Mountain area indicates that the predominant initial process was selective emplacement of  $^{234}\text{U}$  and  $^{230}\text{Th}$  (Rosholt, 1980a). Two separate mechanisms may be responsible for emplacement of  $^{234}\text{U}$  and other daughter products from parent atoms in solution: (1) some of the recoiling nuclei ejected at the pore water-particle interface are imbedded in adjacent grains, and (2) some of the precursors of  $^{234}\text{U}$ ,  $^{234}\text{Th}$  and  $^{234}\text{Pa}$ , and  $^{230}\text{Th}$  are

adsorbed on surfaces of particulate matter at this interface. Beta decay of short-lived  $^{234}\text{Th}$  and  $^{234}\text{Pa}$  leaves some of their daughter  $^{234}\text{U}$  atoms implanted on the particulate matter. These  $^{234}\text{U}$  emplacement atoms are not bound strongly to the solid surfaces and subsequently, over extended periods of time, significant fractions are leached back into the water phase at a rate greater than their disintegration rate ( $2.48 \times 10^5$  yr half life). Gradual leaching of emplaced  $^{234}\text{U}$  is accompanied by the displacement mechanism where  $^{234}\text{U}$  produced by decay of structurally incorporated  $^{238}\text{U}$  is selectively released from mineral surfaces by recoiling alpha-emitting nuclei and by natural etching of recoil tracks. Initial emplacement by recoil-adsorption processes probably is limited by the concentrations of dissolved species and by the sorptive properties of the solids. In contrast, displacement by recoil-leaching is controlled by the concentrations in the solid phase and by the solubility of leached isotopes. Apparently, continuous exposure of leachable  $^{234}\text{U}$  sites during glass alteration and higher uranium concentrations in the solid phases results in eventual domination of the displacement mechanism. The empirical model used includes these parameters of daughter emplacement,  $^{234}\text{U}$  displacement, and uranium-flux factor.

#### Empirical Model

Because of the large number of variables in a system that is completely open with regard to migration of uranium, a rigorous mathematical model based on simple equations for radioactive growth and decay of daughter products cannot be constructed. Instead, an empirical model tested against the results obtained from several alluvial, colluvial, glacial, and eolian deposits of different ages is constructed for solution of uranium-trend ages. The model requires calibration of both the trend slope and the uranium-flux factor based on results from deposits of known age.

The isotopic composition of several samples from the same depositional unit, expressed in activity units, is required for solution of the model. The value from which ages are calculated is the slope of the line representing

$$\frac{\Delta(^{234}\text{U} - ^{238}\text{U})}{\Delta(^{234}\text{U} - ^{230}\text{Th})}$$

A related slope is

$$\frac{\Delta(^{234}\text{U} - ^{238}\text{U})}{\Delta(^{238}\text{U} - ^{230}\text{Th})}$$

The two forms of slope are dependent because

$$\frac{\Delta(^{234}\text{U} - ^{238}\text{U})}{\Delta(^{238}\text{U} - ^{230}\text{Th})} = \frac{\Delta(^{234}\text{U} - ^{238}\text{U})}{\Delta[^{234}\text{U} - ^{230}\text{Th}] - (^{234}\text{U} - ^{238}\text{U})}$$

and this form is used for a computer solution of the age shown in Table 2. The terms  $\Delta(^{238}\text{U} - ^{230}\text{Th})$  and  $\Delta(^{234}\text{U} - ^{230}\text{Th})$  are used rather than  $\Delta(^{230}\text{Th} - ^{238}\text{U})$  and  $\Delta(^{230}\text{Th} - ^{234}\text{U})$  to comply with the convention used by geochronologists where the slope of an isochron increases with age. A diagram (Fig. 1) shows the hypothetical development of a U-trend slope for a three-sample profile. Changes in isotopic composition with time ideally should follow a complex radioactive growth and decay curve; the U-trend slope for the three samples is represented by the tangent to this curve.

The model is based on the empirical assumptions that

$$\begin{aligned} (^{234}\text{U} - ^{238}\text{U}) &= \frac{\lambda_2}{(\lambda_2 - \lambda_0)} e^{-\lambda_0 t} - \frac{\lambda_2}{(\lambda_2 - \lambda_0)} e^{-\lambda_2 t} + e^{-\lambda_2 t} \\ (^{234}\text{U} - ^{230}\text{Th}) &= \frac{-3\lambda_2\lambda_3}{(\lambda_2 - \lambda_0)(\lambda_3 - \lambda_0)} e^{-\lambda_0 t} - \frac{3\lambda_2\lambda_3}{(\lambda_0 - \lambda_2)(\lambda_3 - \lambda_2)} e^{-\lambda_2 t} \\ &\quad - \frac{3\lambda_2\lambda_3}{(\lambda_0 - \lambda_3)(\lambda_2 - \lambda_3)} e^{-\lambda_3 t} - 2e^{-\lambda_2 t} + e^{-\lambda_3 t} \end{aligned}$$

where  $\lambda_0$  is the decay constant of  $F(0) = \ln 2$ /[half period of  $F(0)$ ],  $\lambda_2$  is the decay constant of  $^{234}\text{U}$  ( $0.280 \times 10^{-5}\text{yr}^{-1}$ ), and  $\lambda_3$  is the decay constant of  $^{230}\text{Th}$  ( $0.922 \times 10^{-5}\text{yr}^{-1}$ ). For samples of the same age, the rate of change between parent-daughter activities would be represented by the first derivatives of the above equations:

$$\Delta(^{234}\text{U} - ^{238}\text{U}) = \frac{-\lambda_2 \lambda_0}{\lambda_2 - \lambda_0} e^{-\lambda_0 t} + \frac{\lambda_2 \lambda_2}{\lambda_2 - \lambda_0} e^{-\lambda_2 t} - \lambda_2 e^{-\lambda_2 t}$$

$$\Delta(^{234}\text{U} - ^{230}\text{Th}) = \frac{3\lambda_0 \lambda_2 \lambda_3}{(\lambda_2 - \lambda_0)(\lambda_3 - \lambda_0)} e^{-\lambda_0 t} + \frac{3\lambda_2 \lambda_2 \lambda_3}{(\lambda_0 - \lambda_2)(\lambda_3 - \lambda_2)} e^{-\lambda_2 t}$$

$$+ \frac{3\lambda_2 \lambda_3 \lambda_3}{(\lambda_0 - \lambda_3)(\lambda_2 - \lambda_3)} e^{-\lambda_3 t} + 2\lambda_2 e^{-\lambda_2 t} - \lambda_3 e^{-\lambda_3 t}$$

The slope of the line represented by the quotient of these two equations is used in the model. To accommodate measured isotopic data, the isotopic variations were normalized to  $^{238}\text{U}$  and the exponential terms written in the form of Bateman equations, where

$$\frac{Y}{X} = \frac{\Delta(^{234}\text{U} - ^{238}\text{U})/^{238}\text{U}}{\Delta(^{234}\text{U} - ^{230}\text{Th})/^{238}\text{U}} = \frac{C_1 e^{-\lambda_0 t} + C_2 e^{-\lambda_2 t}}{C_3 e^{-\lambda_0 t} + C_4 e^{-\lambda_2 t} + C_5 e^{-\lambda_3 t}}$$

$$C_1 = \frac{-\lambda_0 \lambda_2}{\lambda_2 - \lambda_0}; \quad C_2 = \frac{\lambda_2 \lambda_2}{\lambda_2 - \lambda_0} - \lambda_2; \quad C_3 = \frac{3\lambda_0 \lambda_2 \lambda_3}{(\lambda_2 - \lambda_0)(\lambda_3 - \lambda_0)};$$

$$C_4 = \frac{3\lambda_2 \lambda_2 \lambda_3}{(\lambda_0 - \lambda_2)(\lambda_3 - \lambda_2)} + 2\lambda_2; \quad C_5 = \frac{3\lambda_2 \lambda_3 \lambda_3}{(\lambda_0 - \lambda_3)(\lambda_2 - \lambda_3)} - \lambda_3.$$

These are empirical model equations and the numerical constants in the coefficients preceding the exponential terms were determined by computer synthesis to provide a model with the best fits for deposits of known age. The alternative uranium-trend slope is represented by

$$\frac{Y}{X - Y} = \frac{\Delta(^{234}\text{U} - ^{238}\text{U})/^{238}\text{U}}{\Delta(^{238}\text{U} - ^{230}\text{Th})/^{238}\text{U}}$$

and is used for computer solution of the age. An example of this linear trend is shown in Figure 2.

An additional parameter in the uranium-trend plot is the intercept of the slope line on the X-axis,  $x_i$ , represented by

$$y = mx + b$$

$$x_i = -b/m$$

where  $m$  is the measured slope of the line,  $b$  is the intercept on the Y-axis, and  $x_i$  is the intercept on the X-axis. The value of  $x_i$  is used to obtain time calibration for the uranium-trend model.

A different plot of the isotopic data can be constructed when the  $^{238}\text{U}/^{232}\text{Th}$  ratios of the samples are plotted on the X-axis versus the  $^{230}\text{Th}/^{232}\text{Th}$  ratios plotted on the Y-axis as shown in Figure 3. This thorium plot is similar to the isochron plot used by Allegre and Condomines (1976) for dating of young volcanic rocks. However, it is not used to determine ages in the manner used by Allegre and Condomines because the initial conditions did not fit their model which is designed for volcanic rocks, nor does their closed-system requirement apply. Instead, it is used only to determine if all the samples included in the uranium-trend line describe a reasonable linear array on the thorium plot, and thus serves as a useful check to determine if all samples belong in the same deposition unit.

The half period of  $F(0)$  and its decay constant,  $\lambda_0$ , are strictly empirical values which allow selection of the proper exponential coefficient in the equation for the uranium-trend model. For depositional units of unknown age, a method is required to determine the  $\lambda_0$  value to be used in the equation; this is done with a calibration curve based on  $\lambda_0$  determined for units of known age. For this calibration, the quantity  $x_i$  is plotted against the half period of  $F(0)$  on a log-log plot shown in Figure 4. The calibration curve is determined by selecting the proper  $\lambda_0$  values that will yield the known ages for deposition units using the model equation. The measured  $x_i$  values of known-age deposits are used for calibration and these values are plotted against the half periods of  $F(0)$  equivalent to their  $\lambda_0$  values required, in the empirical equation, to obtain the correct ages for the deposits. The solution of the empirical equation, using any given half period of  $F(0)$  yields an array of uranium-trend slopes representing various ages. Figure 5 shows an example of the slopes for various ages calculated for half periods of 100,000 and 600,000 years.

## Calibration

Analyses of deposits of known age are required for time calibration of the empirical model. The quantity, half period of  $F(0)$ , is one variable used for calibration of the model. The value,  $x_i$ , is the measured parameter in the calibration. A half period of  $F(0)$  for a given suite of samples is obtained from the calibration plot (Fig. 4) using the  $x_i$  value determined from the uranium-trend plot. The known-age deposits used for calibration points that define the line also are indicated on Figure 4.

Four primary calibration points represented by reliable age determinations based on different radiometric dating techniques were used for time correlations. The uranium-trend model parameters for each of 12 calibration units are included in Table 1. These calibration units are:

(1) The radiocarbon date of 12 Ka (Frye, 1973) was used for calibration with analyzed samples from loess of late Wisconsin age in Minnesota (units 2 and 3, Table 1). A secondary calibration with Piney Creek Alluvium from the Kassler quadrangle, Colorado (unit 1) was used because of the reliability of an estimated age of about 5 Ka for this deposit (Scott, 1963, p. 52). A secondary calibration point at about 12 Ka for till of Pinedale age at Peaceful Valley, Colorado (unit 5).

(2) The obsidian-hydration date of 140 Ka with the correlation to the K-Ar age for Bull Lake deposits near West Yellowstone, Montana (Pierce and others, 1976), was used initially for calibration of end moraine and loess, of Bull Lake age in the West Yellowstone area, listed in Table 1 as units 8 and 9, respectively. Revision of the obsidian hydration data from 140 to 150 Ka was made recently by Pierce (1979, p. F24). Secondary calibration points for Bull Lake age deposits are represented by till in the Allen's Park area, Colorado (unit 6), and till sampled at Fremont Ditch, near Pinedale, Wyoming (unit 7). Thus an estimated age of deposition of about  $150 \pm 15$  Ka is used to define the calibration line where Bull Lake age correlations (units 6-10) give uranium-trend ages varying from 130 to 190 Ka.

(3) Correlation with the K-Ar age of 0.6 Ma for the Lava Creek Tuff eruption (J. D. Obradovich, written commun., 1973), which also produced the Pearlette type 0 ash or Lava Creek ash bed, was used for calibration of zeolitized Pearlette type 0 ash in tuff A, Lake Tecopa, California (unit 11, Table 1). A fission-track age of 0.6 Ma for this ash (Naeser and others, 1973) confirms the time calibration.

(4) Correlation with the K-Ar age of 0.73 Ma for Bishop Tuff (Dalrymple and others, 1965) was used for calibration of tuff B, Lake Tecopa. A fission-track age of 0.74 Ma for this tuff (Izett and Naeser, 1976) confirms the K-Ar age. Although no K-Ar or fission-track age determinations were made on samples from deposits in Lake Tecopa, the ash layers in tuff A and tuff B have been correlated with Pearlette type O ash and Bishop Tuff, respectively, by Izett and others (1970). Tuff C (unit 13) has been correlated with Pearlette type B ash or Hucklebury Ridge ash by Izett (oral commun., 1979). The same correlations for these ashes was made by Sarna-Wojcicki and others (1980).

#### EXPERIMENTAL PROCEDURES

It should be stressed that all procedures should be performed in a uniform and reproducible manner, and accuracy in analyses is important because of the emphasis the model places on the small isotopic variation between samples in a deposit.

#### Sample Collection, Preparation, and Chemical Procedures

To obtain a uranium-trend date, several samples, about 1 kg each, should be collected from a vertical section of each depositional unit; however, the required number of samples for a reliable trend plot depends on the variation in ratios of uranium and thorium that define the trend line. The minimum number of samples needed will not be known until analyses are completed; therefore, subdividing the unit into a larger number of samples usually will increase the likelihood of better defining the uranium-trend line. A minimum of three samples is required but it is desirable to have at least five in a given sampling unit to determine a reliable slope. A problem is that it is not always possible to establish, in the field, the exact boundary between different depositional units. To help alleviate this problem, collection of a larger number of samples is required in some sections. In soils, subdivision of samples by soil horizon is appropriate. Differences in sediment mineralogy and particle size also are good field criteria for selecting samples that will give a suitable spread of values to define a linear trend. Channel sampling of depositional units exposed in a trench or at least from a relatively fresh, well-exposed outcrop is preferable.

If the sample contains pebbles and larger fragments, the size fraction that will pass through a 10-mesh sieve is retained for analysis, pulverized to

less than 0.2-mm size, and homogenized. The whole sample that is less than 10 mesh is used for analysis. A schematic outline of the steps in the separation procedure is shown in Figure 6.

A sample aliquot weighing 3 to 8 grams, depending on estimated uranium content, is heated to 900°C in a muffle furnace to convert calcium carbonate to calcium oxide and to decompose organic matter. The cooled sample is reweighed to determine loss on ignition, rinsed into a teflon evaporating dish and aliquots of standardized  $^{236}\text{U}$  and  $^{229}\text{Th}$  solutions are added. Each covered sample is decomposed with nitric and hydrofluoric acids and, under heat lamp, taken to dryness overnight. Evaporation to dryness following addition of nitric and hydrofluoric acids is repeated three times. The residue is dissolved in approximately 100 ml of hot 6F hydrochloric acid; retention at boiling point for up to one hour may be required to dissolve calcium fluoride. Small amounts of residue usually remain, consisting of partially decomposed resistate minerals; no attempt is made to separate the residue from the hydrochloric acid solution. The cooled solution is added to a Dowex 1-X8 (100-200 mesh) anion exchange column (15 cc volume, 5 cm height) in the chloride form. Thorium does not form stable chloride anionic complexes; hence, it passes directly through the column while uranium and ferric chloride complexes are adsorbed (Krauss and others, 1956). The ion exchange column is washed three times with 15 ml of 6F hydrochloric acid, and all of the solution that passed through the column is retained for subsequent thorium purification. Uranium is recovered from the column in a separate Teflon beaker via elution with 50 ml of water. The aqueous solution is evaporated to dryness, dissolved in a small volume of 7F nitric acid, mixed with 25 ml of a saturated solution of magnesium nitrate, transferred to 125 ml separatory funnel, and separated from iron by solvent extraction with an equal volume of methyl isobutyl ketone (Hexone). The organic phase is retained and washed with an additional equal volume of magnesium nitrate solution. Uranium is recovered from the organic phase by back extraction twice with water, and evaporated to dryness. Uranium is further purified from any residual iron and magnesium nitrate by anion exchange with a Biorad 1-X8 (100-200 mesh) column (4 cc volume, 9 cm height) in the nitrate form using 7F nitric acid for loading and washing, and water for elution. To assure removal of any residual thorium, the residue from the evaporated uranium solution is dissolved in a small drop of hydrochloric acid and processed by anion exchange with a Biorad

1-X8 (100-200 mesh) column (4 cc volume, 9 cm height) in the chloride form. The purified uranium, following evaporation to dryness, is dissolved in a microdrop of hydrochloric acid, mixed with 1.5 ml of 2F ammonium chloride electrolyte solution, adjusted to pH 6, transferred to a small volume Teflon plating apparatus, and electroplated onto a disc suitable for alpha-spectrometer counting; the resulting electrodeposit of uranium is 1.25 cm diameter. Platinum discs and a thin circular platinum electrode are used for uranium electrodeposition requiring about 20 minutes of plating at an initial current of 1.8 amps decreasing to 0.4 amp at completion of deposition. Several drops of ammonium hydroxide are added to electrolyte solution before the current is shut off, and the disc is flame dried for subsequent counting.

The hydrochloric acid solution containing thorium is evaporated to 50 ml volume, and thorium is coprecipitated with aluminum after the addition of ammonium hydroxide to obtain alkaline solution. The precipitate is centrifuged, supernatant discarded, washed with distilled water, centrifuged, supernatant discarded, and the precipitate is dissolved in 20 ml of 7F nitric acid. This solution is diluted to 80 ml with distilled water, and thorium is coprecipitated from hot solution with zirconium pyrophosphate (Rosholt, 1957). The precipitate is formed after addition of 20 mg Zr/0.2 ml from a solution of ultrapure zirconyl chloride reagent and 8 ml of 0.1F sodium pyrophosphate solution. The precipitate is centrifuged, supernate discarded, washed with distilled water, centrifuged, supernate discarded, and the zirconium pyrophosphate precipitate is transferred with water to a 50 ml beaker and dissolved with the addition of 1 gram of oxalic acid after heating. Ultrapure lanthanum nitrate (15 mg La/10 ml) is added to precipitate lanthanum oxalate carrier and purify thorium from zirconium. The precipitate is centrifuged, supernate discarded, and the lanthanum oxalate precipitate is dissolved in 2 ml of 7F nitric acid. The dissolved precipitate is added to a previously prepared and conditioned Biorad 1-X8 anion exchange column (6 cc volume, 13 cm height) in nitrate form. Anionic nitrate complexes of thorium are adsorbed on the anion exchange resin to assure complete sorbtion of thorium, flow in the column is halted for about one hour after initial wash volume is added but prior to its passage through the column and thorium is separated from lanthanum. The column is washed four times with 6 ml of 7F nitric acid, and thorium is recovered via elution with 20 ml of 0.5F hydrochloric acid. After evaporation to dryness in a Teflon beaker, the

thorium is purified from any residual lanthanum and uranium by solvent extraction, following dissolution in 0.3 ml of 0.08F nitric acid and removal from the beaker. Approximately 0.15 ml of TTA (thenoyl trifluoro acetone) is added to the solution in a 7 ml centrifuge tube, agitated thoroughly, and thorium is extracted into the organic phase. The organic phase is removed from the aqueous phase with a micropipette and slowly evaporated on a stainless steel disc under a heat lamp. The disc is flame dried and the TTA extraction/evaporation procedure is repeated. The disc is flame dried again and placed in the alpha spectrometer for counting.

#### Isotopic Measurements and Counting Error

Uranium and thorium separates are measured, individually, in high-resolution alpha spectrometer units and a large-capacity multichannel analyzer with multiple input capability. Partially depleted silicon surface barrier detectors are used in the spectrometer units. A block diagram of a typical alpha-particle spectroscopy system is shown by Chanda and Deal (1970); however, liquid nitrogen-cooled cryostat units are not required for our detectors. A typical alpha-particle spectrum for each of these separates is shown in Figure 7.

A minimum of 10,000 counts in the integrated portion of each alpha-energy peak normally is accumulated for each measurement. For defining linear trends, a uranium sample is counted four separate times and averaged, and a thorium sample is counted three separate times and averaged. The  $^{238}\text{U}/^{236}\text{U}$  activity ratio is used to determine the uranium concentration by radioisotope dilution using a  $^{236}\text{U}$  spike calibrated with a standard uraninite sample solution (Rosholt, 1984). The  $^{232}\text{Th}/^{229}\text{Th}$  activity ratio is used to determine thorium concentration. The  $^{230}\text{Th}/^{229}\text{Th}$  activity ratio is used to determine  $^{230}\text{Th}$  content by radioisotope dilution with a  $^{229}\text{Th}$  spike calibrated with a standard uraninite sample solution. The concentrations of  $^{238}\text{U}$  and  $^{230}\text{Th}$  in the standard uraninite solution are calibrated with NBS 950 standard uranium. Activity ratios of  $^{234}\text{U}/^{238}\text{U}$  and  $^{230}\text{Th}/^{232}\text{Th}$  are measured directly from the spectra; activity ratios of  $^{230}\text{Th}/^{238}\text{U}$  and  $^{238}\text{U}/^{232}\text{Th}$  are calculated from data obtained in both spectra where

$$\frac{^{230}\text{Th}}{^{238}\text{U}} = \frac{\mu\text{g equiv. } ^{230}\text{Th}}{\mu\text{g } ^{238}\text{U}}$$

$$\frac{^{238}\text{U}}{^{232}\text{Th}} = \frac{^{230}\text{Th}/^{232}\text{Th}}{^{230}\text{Th}/^{238}\text{U}}$$

$$\frac{^{234}\text{U} - ^{238}\text{U}}{^{238}\text{U}} = \frac{^{234}\text{U}}{^{238}\text{U}} - 1$$

$$\frac{^{238}\text{U} - ^{230}\text{Th}}{^{238}\text{U}} = 1 - \frac{^{230}\text{Th}}{^{238}\text{U}}$$

Uranium isotopic ratios determined by four separate measurements, each counted with a different detector, indicate the standard deviations in each of the isotopic ratios exceeds the value of the errors calculated from counting statistics. Thus, accumulating integrated alpha peaks of uranium isotopes that are greater than 10,000 counts per peak in each spectrum, the standard deviation of the four measurements is used to obtain a  $2\sigma$  error value. The same procedure is used to obtain the  $2\sigma$  error value for thorium isotopic ratios based on three separate counts. Significantly smaller errors calculated by counting statistics than those calculated by standard deviations apparently are due to differences in the spectral shape and the area over which a peak is integrated, and to slight variations in geometry and electronic components when separate spectrometer units are used for each measurement.

The computer program used to calculate the slope and uncertainties in the slope of the linear trend specifies that  $2\sigma$  error values should be used to obtain a York fit of the line to the measured data. Typically the following  $2\sigma$  values were determined from standard deviations for several measurements and these values are used for the counting errors of the ratios required for plots:

<u>Ratio</u>	<u><math>2\sigma</math> error (percent)</u>
$^{234}\text{U}/^{238}\text{U}$	3.2
$^{230}\text{Th}/^{238}\text{U}$	4.2
$^{230}\text{Th}/^{232}\text{Th}$	2.8
$^{238}\text{U}/^{232}\text{Th}$	5.2

## Linear Trend Plots and Linear Regression Calculations

A Hewlett-Packard 9830/9862 computer/plotter<sup>1</sup> is used for X-Y plots of both the uranium-trend data and the thorium-index data. The program, supplied by Ludwig (1979), is also used to calculate fitting of the linear trends. After the data are plotted, a least squares regression line is calculated using a modified York (1969) fit, which assumes error in both X and Y parameters and that all scatter from a straight line is due to normally distributed analytical error. The program requires that  $2\sigma$  analytical errors are included with each isotopic ratio used to complete the data array. The resulting error in the calculated straight line is  $1\sigma$  including the observed scatter. The uncertainty in the regression line is asymmetric except at low values. To correct this asymmetry, the uncertainty of the angle,  $\theta$ , of the line with the X-axis also is calculated, so that the plus and minus slope errors are angularly symmetric about the best-fit line. Equations for determining the angular uncertainty are given by Ludwig (1980).

$$\theta = \tan^{-1}S$$

$$\Delta\theta = \Delta_S \cos^2(\tan^{-1}S)$$

$$S' = \{\tan^{-1}S + \Delta\theta\} + \tan[(\tan^{-1}S) - \Delta\theta] / 2$$

$$\Delta_S' = \tan[(\tan^{-1}S) \pm \Delta\theta] - S$$

where  $S$  is the slope and  $\theta$  is the angle of the linear regression line,  $\Delta\theta$  is its angular uncertainty,  $S'$  is the angularly symmetric slope, and  $\Delta_S'$  is the angularly symmetric uncertainty of the slope. The angle,  $\theta$ , should be expressed in radians to obtain the term  $\Delta\theta$  which is converted to degrees to obtain  $S'$ . The value of  $S'$  is used to obtain the uranium-trend age from the computer solution of the empirical equation shown in Table 2.

<sup>1</sup>Use of trade names is for descriptive purposes only and does not imply endorsement by the U. S. Geological Survey.

## RESULTS

An open system empirical model for uranium-trend dating must be calibrated, as discussed earlier, by analysis of several depositional units of known age that extend over a major part of the time range allowed by the model. Results on primary calibration units are included in chapter 2 which is part of the compilation containing a large amount of  $^{238}\text{U}$ - $^{234}\text{U}$ - $^{230}\text{Th}$  data required to assess the reliability of uranium-trend dating. Several other chapters describe the work on 13 deposits from the San Joaquin and Sacramento Valleys, California, 10 deposits from the Rio Grande and Pecos Valleys, New Mexico, 40 deposits from the Nevada Test Site area, Nevada, 14 marine-type deposits on the southeastern Atlantic Coastal Plain, and marine terrace deposits from California and Barbados. A separate chapter is devoted to each area studied because of the number of coauthors that have been involved in this broad investigation, and because of the geologic complexities of each study area.

The key parameters for the uranium-trend model are (1) the slope of the linear regression for the  $^{238}\text{U}$ - $^{234}\text{U}$ - $^{230}\text{Th}$  data, (2) the intercept on the X-axis of this plot, (3) the half period of  $F(0)$  obtained from the calibration curve, and (4) the calculated age. These parameters for the primary and secondary calibration units used for the model are shown in Table 1.

## SUMMARY

A variation of uranium-series dating called uranium-trend dating has been tested extensively over the past several years to determine its reliability in estimating the time of deposition of Quaternary sediments. In these sorts of materials, an open system dating technique must be used. Because of the large number of variables in a system which is completely open with regard to migration of uranium and its resultant trail of long-lived daughter products, a rigorous mathematical model based on simple equations for radioactive growth and decay of daughter products cannot be constructed. Instead, an empirical model that is based on analyses of alluvial, colluvial, glacial, eolian, and altered volcanic ash deposits, ranging in age from 5 to 730 Ka, is used to determine uranium-trend ages. The model requires time calibration based on results from depositional units of known age. A radiocarbon date of 12 Ka was used for loess of late Wisconsin age; an obsidian hydration date of 150 Ka with correlation to K-Ar age was used to calibrate Bull Lake deposits in

Montana, Wyoming, and Colorado; and K-Ar ages of 600 and 730 Ka for Pearlette type O ash or Lava Creek ash and Bishop Tuff, respectively, were used to calibrate zeolitized volcanic ash beds (tuff A and tuff B, respectively) from Lake Tecopa, California.

Analyses of isotopic abundances of  $^{238}\text{U}$ ,  $^{234}\text{U}$ ,  $^{230}\text{Th}$ , and  $^{232}\text{Th}$  in several samples from the same depositional unit are required for solution of the model. Whole-rock samples are used and isotopic concentrations are determined by radioisotope dilution techniques and alpha spectrometer measurements. Results of the analyses are presented graphically where  $^{238}\text{U}/^{232}\text{Th}$  vs.  $^{230}\text{Th}/^{232}\text{Th}$  is used for the thorium-index plot, and  $(^{238}\text{U}-^{230}\text{Th})/^{238}\text{U}$  vs.  $(^{234}\text{U}-^{238}\text{U})/^{238}\text{U}$  is used for the uranium-trend plot. The data ideally yield linear relationships, and the measured slope of the uranium-trend line changes in a systematic way with increasing age of the deposit. The rate of change of slope is determined by  $F(0)$ , a factor whose physical significance is not well understood, but relates to movement of mobile-phase uranium through the deposit. The half-period of  $F(0)$  is estimated from the calibration curve established by uranium-trend lines for depositional units of known age. The starting point for the uranium-trend clock was the time of deposition of the sediment rather than initiation of soil development. In summary, the key parameters for the uranium-trend model are (1) the slope of the linear regression for the  $^{238}\text{U}-^{234}\text{U}-^{230}\text{Th}$  data, (2) the intercept on the X-axis of this plot, (3) the half period of  $F(0)$  obtained from the calibration curve, and (4) the calculated age.

Based on results of about 100 uranium-trend ages, the method has a potential accuracy, at best, of about  $\pm 10$  percent for deposits older than 100,000 years. The uncertainty in the slope may be greater depending on scatter of data points and spread between points along a linear trend. Percent errors in the ages are not symmetric throughout the range and they are greater for both younger ( $<60,000$  years) and older ( $>600,000$  years) deposits. Depositional units that have initially low uranium concentrations produce more accurate trend lines because the trail of daughter products left by the uranium migration flux (mobile phase) overrides, to a greater degree, the products of original uranium content (fixed phase) that tends to be locked into parent material.

Materials that have a potential for dating are alluvial, lacustrine, marine, eolian, and glacial deposits, and volcanic-ash deposits if they have

been altered appreciably to zeolites or clays. It also appears feasible to date the formation of caliche when calcium carbonate is the predominant (>50%) component in the surficial deposit, gypsiferous spring deposits, and dissolution residues in older halite formations (Szabo and others, 1980). The latter studies suggest that geochemical replacement processes such as those represented by carbonate-rich residues could be investigated further to evaluate their potential for uranium-trend dating.

Because alluvial and glacial deposits are key elements in most Pleistocene successions, dated chronosequences from different areas and climatic regimes should be compared by this technique. To learn more about the age relationships between Pleistocene marine deposits and those of the continental interior, well-described marine terraces should be dated and compared with deposits of continental origin.

## REFERENCES CITED

- Allegre, C. J., and Condomines, M., 1976, Fine chronology of volcanic processes using  $^{238}\text{U}/^{230}\text{Th}$  systematics: *Earth and Planetary Science Letters*, v. 28, p. 395-406.
- Chanda, R. N., and Deal, R. A., 1970, Catalogue of semiconductor alpha-particle spectra: USAEC Report IN-1261, p. 159.
- Dalrymple, G. B., Cox, Allan, and Doell, R. R., 1965, Potassium-argon age and paleomagnetism of the Bishop Tuff, California: *Geol. Soc. America Bull.*, v. 76, p. 665-674.
- Fleischer, R. L., 1980, Isotopic disequilibrium of uranium. Alpha-recoil damage and preferential solution effects: *Science*, v. 207, p. 979-981.
- Fleischer, R. L., 1983, Theory of alpha recoil effects on radon release and isotopic disequilibrium: *Geochimica et Cosmochimica Acta*, v. 47, p. 779-784.
- Fleischer, R. L., and Raabe, O. G., 1978, Recoiling alpha-emitting nuclei. Mechanisms for uranium-series disequilibrium: *Geochimica et Cosmochimica Acta*, v. 42, p. 973-978.
- Frye, J. C., 1973, Pleistocene succession of the central interior United States: *Quaternary Research*, v. 3, p. 275-283.
- Hansen, R. O., 1965, Isotopic distribution of uranium and thorium in soils weathered from granite and alluvium: Ph.D. dissertation, Univ. of Calif., Berkeley, p. 135.
- Hansen, R. O., and Huntington, G. L., 1969, Thorium movements in morainal soils of the High Sierra, California: *Soil Science*, v. 108, p. 257-265.
- Hansen, R. O., and Stout, P. R., 1968, Isotopic distributions of uranium and thorium in soils: *Soil Science*, v. 105, p. 44-50.
- Ivanovich, M., and Harmon, R. S., 1982, *Uranium Series Disequilibrium: Applications to Environmental Problems*, Clarendon Press, Oxford, 571 p.
- Izett, G. A., and Naeser, C. W., 1976, Age of the Bishop Tuff of eastern California as determined by the fission-track method: *Geology*, v. 4, p. 587-590.
- Izett, G. A., Wilcox, R. E., Powers, H. A., and Desborough, G. A., 1970, The Bishop ash bed, a Pleistocene marker bed in the western United States: *Quaternary Research*, v. 1, p. 122-132.
- Kigoshi, K., 1971, Alpha-recoil  $^{234}\text{Th}$ : dissolution into water and the  $^{234}\text{U}/^{238}\text{U}$  disequilibrium in nature: *Science*, v. 173, p. 47-48.

- Knauss, K. and Ku, T. L., 1980, Desert varnish: Potential for age dating via uranium-series isotopes: *J. Geology*, v. 88, p. 95-100.
- Krauss, K. A., Moore, G. E., and Nelson, F., 1956, Anion exchange studies XXI. Thorium (IV) and uranium (IV) in hydrochloric acid separation of thorium, protactinium, and uranium: *J. American Chem. Soc.*, v. 78, p. 2692-2695.
- Ku, T. L., 1976, The uranium-series methods of age determination: *Annual Rev. Earth and Planetary Science Letters*, v. 4, p. 347-379.
- Ku, T. L., Bull, W. B., Freeman, S. T., and Knauss, K. G., 1979,  $\text{Th}^{230}$ - $\text{U}^{234}$  dating of pedogenic carbonates in gravelly desert soils of Vidal Valley, Southeastern California: *Geol. Soc. America Bull.*, v. 90, p. 1063-1073.
- Ludwig, K. R., 1979, A program in Hewlett-Packard BASIC for X-Y plotting and line-fitting of isotopic and other data: *U. S. Geol. Survey Open File Report*, 79-1641, 28 p.
- Ludwig, K. R., 1980, Calculation of uncertainties of U-Pb isotope data: *Earth Planet. Sci. Letters*, v. 46, p. 212-220.
- Megumi, K., 1979, Radioactive disequilibrium of uranium and actinium series nuclides in soil: *J. Geophys. Research*, v. 84, p. 3677-3682.
- Naeser, C. W., Izett, G. A., and Wilcox, R. E., 1973, Zircon fission-track ages of Pearlette family ash beds in Meade County, Kansas: *Geology*, v. 1, p. 187-189.
- Osmond, J. K., and Cowart, J. B., 1976, The theory and use of natural uranium isotopic variations in hydrology: *Atomic Energy Review*, v. 14, no. 4, p. 621-679.
- Pierce, K. L., 1979, History and dynamics of glaciation in the northern Yellowstone National Park area: *U.S. Geological Survey Prof. Paper* 729-F, p. F1-F90.
- Pierce, K. L., Obradovich, J. D., and Friedman, I., 1976, Obsidian hydration dating and correlation of Bull Lake and Pinedale glaciations near West Yellowstone, Montana: *Geol. Soc. America Bull.*, v. 87, p. 702-710.
- Rosholt, J. N., 1957, Quantitative radiochemical methods for determination of the sources of natural radioactivity: *Anal. Chem.*, v. 29, p. 1398-1408.
- Rosholt, J. N., 1980a, Uranium and thorium disequilibrium in zeolitically altered rock: *Nuclear Technology*, v. 57, p. 143-146.
- Rosholt, J. N., 1980b, Uranium-trend dating of Quaternary sediments: *U.S. Geol. Survey Open-File Report* 80-1087, 65 p.

- Rosholt, J. N., 1983, Isotopic composition of uranium and thorium in crystalline rocks: Jour. Geophys. Res., v. 88, No. B9, p. 7315-7330.
- Rosholt, J. N., 1984, Isotope dilution analyses of uranium and thorium in geologic samples using  $^{236}\text{U}$  and  $^{229}\text{Th}$ : Nuclear Instr. and Methods, v. 223, p. 572-576.
- Rosholt, J. N., Doe, B. R., and Tatsumoto, M., 1966, Evolution of the isotopic composition of uranium and thorium in soil profiles: Geol. Soc. America Bull., v. 77, p. 987-1004.
- Sarna-Wojcicki, A. M., Bowman, H. W., Meyer, C. E., Russell, P. C., Asaro, F., Michael, H., Rowe, J. J., Baedeker, P. A., and McCoy, G., 1980, Chemical analyses, correlations, and ages of late Cenozoic tephra units of east-central and southern California: U.S. Geol. Survey Open-File Report 80-231, 57p.
- Stuckless, J. S., and Ferreira, C. P., 1976, Labile uranium in granite rocks, in Internation Symposium on Exploration of Uranium Ore Deposits, Proc., Vienna: Internat. Atomic Energy Agency Tech. Rpts. Ser., p. 717-730.
- Szabo, B. J., 1969, Uranium-series dating of Quaternary successions: Union Internat. for Quaternary Studies, VIII INQUA Conf., Paris, p. 941-949.
- Szabo, B. J., Gottschall, W. C., Rosholt, J. N., and McKinney, C. R., 1980 Uranium series disequilibrium investigations related to the WIPP site, New Mexico: U.S. Geol. Survey Open-File Report 80-879, 22p.
- York, D., 1979, Least squares fitting of a straight line with correlated errors: Earth Planet. Sci. Letters, v. 5, 320-324.
- Zielinski, R. A., Lindsey, D. A., and Rosholt, J. N., 1980, The distribution and mobility of uranium in glassy and zeolitized tuff, Keg Mountain area, Utah, U.S.A.: Chemical Geology, v. 29, p. 139-162.

Table 1. Uranium-trend model parameters and ages of deposition units

Unit	Description of deposit	U-trend slope	X-intercept	Half period of F(0) (Ka)	Adjusted* U-trend age (Ka)
1	PC unit, Piney Creek alluvium, Kassler quadrangle, CO.	+0.045	-2.74	68	5 ± 20
2	WF unit, late Wisconsin loess, Wabasha County, MN.	+ .050	+1.43	70	7 ± 5
3	FF unit, late Wisconsin loess, Fillmore County, MN.	+ .082	+ .671	72	12 ± 15
4	K unit, Wisconsin till, Mower County, MN.	+ .104	+ .596	76	15 ± 15
5	MSV1 unit, slope wash (upper part) till of Pinedale glaciation (lower part) Peaceful Valley, CO	+ .064 + .047	- .430 - .061	100 620	12 ± 14 60 ± 50
6	NSV2 unit, till of Bull Lake, glaciation, Allens Park, CO.	+ .134	- .119	550	130 ± 80
7	FD unit, Bull Lake moraine, Sublette County, Wyo.	+ .225	- .182	440	160 ± 50
8	P78 unit, Bull Lake moraine, West Yellowstone, MT.	+ .114	- .009	720	150 ± 100
9	P183 lower unit, Bull Lake loess, West Yellowstone, MT.	+ .138	- .055	630	160 ± 50
10	P184 lower unit, Bull Lake moraine, West Yellowstone, MT.	+ .177	+ .031	670	190 ± 90
11	Tuff A unit, Lake Tecopa, Inyo County, CA.	- .482	+ .118	550	600 ± 60
12	Tuff B unit, Lake Tecopa, Inyo County, CA.	- .386	+ .033	660	740 ± 100
13	Tuff C unit, Lake Tecopa, Inyo County, CA.	<- .347	- .109	560	>800

\*Ages are modified slightly from those derived by independent methods to produce a smooth curve in Figure 4.

Table 2. Computer solution of Empirical Equation<sup>1</sup>  
 Half period of F(0) = 600 Ka  $\lambda_0 = 0.11552 \times 10^{-5} \text{yr}^{-1}$

Age (Ka)	$C_1 e^{-\lambda_0 t} + C_2 e^{-\lambda_2 t}$	$C_3 e^{-\lambda_0 t} + C_4 e^{-\lambda_2 t} + C_5 e^{-\lambda_3 t}$	$\frac{\Delta(^{234}\text{U}-^{238}\text{U})}{\Delta(^{234}\text{U}-^{230}\text{Th})}$	$\frac{\Delta(^{234}\text{U}-^{238}\text{U})}{\Delta(^{238}\text{U}-^{230}\text{Th})}$	Age (Ka)
10	-0.00317	-0.3685	0.0086	0.0087	10
20	- .00621	- .3728	.0167	.0170	20
40	- .01195	- .3750	.0319	.0329	40
60	- .01724	- .3702	.0466	.0488	60
80	- .02210	- .3602	.0614	.0654	80
100	- .02657	- .3460	.0768	.0832	100
120	- .03066	- .3289	.0932	.1028	120
140	- .03440	- .3097	.1111	.1250	140
160	- .03782	- .2890	.1309	.1506	160
180	- .04093	- .2675	.1530	.1807	180
200	- .04375	- .2455	.1782	.2169	200
220	- .04630	- .2234	.2072	.2614	220
240	- .04861	- .2016	.2411	.3177	240
260	- .5067	- .1801	.2812	.3913	260
280	- .05252	- .1593	.3297	.4918	280
300	- .05416	- .1391	.3892	.6372	300
320	- .05560	- .1197	.4643	.8666	320
340	- .05687	- .1012	.5618	1.2819	340
360	- .05797	- .0836	.6935	2.2623	360
380	- .05892	- .0668	.8813	7.4218	380
400	- .05972	- .0510	1.1701	-6.8781	400
420	- .06038	- .0361	1.6714	-2.4893	420
440	- .06092	- .0221	2.7547	-1.5699	440
460	- .06235	- .0089	6.8271	-1.1716	460
480	- .06166	.0032	-18.7483	-.9494	480
500	- .06187	.0147	- 4.1991	-.8077	500
520	- .06199	.0253	- 2.4423	-.7095	520
540	- .06203	.0352	- 1.7589	-.6375	540
560	- .06198	.0444	- 1.3955	-.5826	560
580	- .06186	.0528	- 1.1702	-.5392	580
600	- .06168	.0606	- 1.0169	-.5042	600
620	- .06143	.0678	- .9059	-.4753	620
640	- .06112	.0743	- .8219	-.4511	640
660	- .06076	.0803	- .7562	-.4306	660
680	- .06035	.0858	- .7033	-.4129	680
700	- .05990	.0907	- .6600	-.3976	700
720	- .05941	.0952	- .6283	-.3842	720
740	- .05888	.0992	- .5932	-.3723	740
760	- .05832	.1028	- .5669	-.3618	760
780	- .05772	.1060	- .5441	-.3524	780
800	- .05711	.1089	- .5242	-.3439	800
820	- .05646	.1114	- .5067	-.3363	820
840	- .05580	.1136	- .4912	-.3294	840
860	- .05512	.1154	- .4773	-.3231	860
880	- .05442	.1170	- .4649	-.3173	880
900	- .05370	.1184	- .4536	-.3121	900
920	- .05298	.1194	- .4434	-.3072	920
940	- .05224	.1203	- .4342	-.3027	940
960	- .05149	.1209	- .4257	-.2986	960
980	- .05074	.1214	- .4180	-.2948	980
1000	- .04998	.1216	- .4108	-.2912	1000

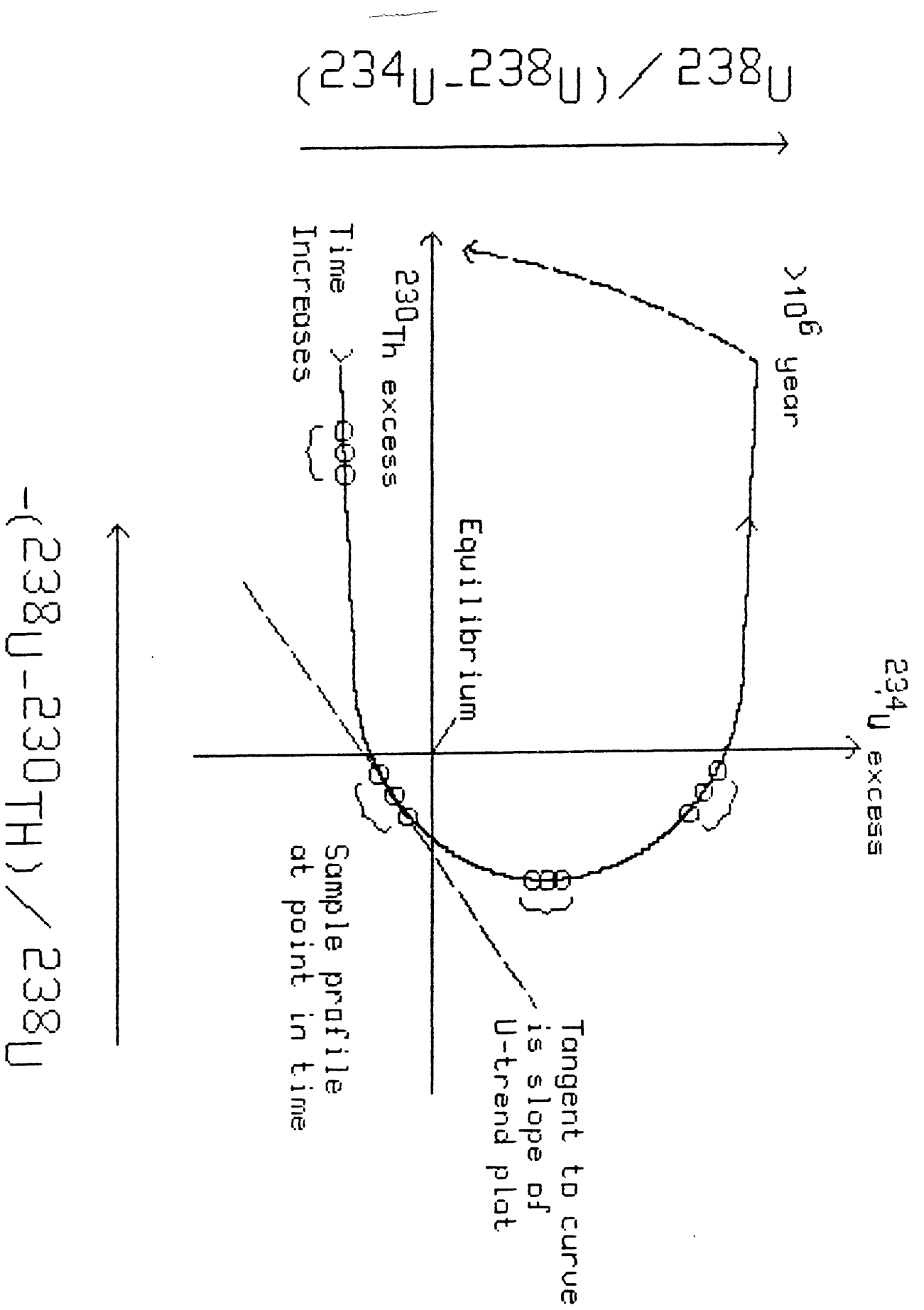


Figure 1. Hypothetical development of  $^{234}\text{U}$ - $^{230}\text{Th}$  disequilibrium for U-trend slope of three-sample profile.

$$\frac{(^{234}\text{U}-^{238}\text{U})}{^{238}\text{U}}$$

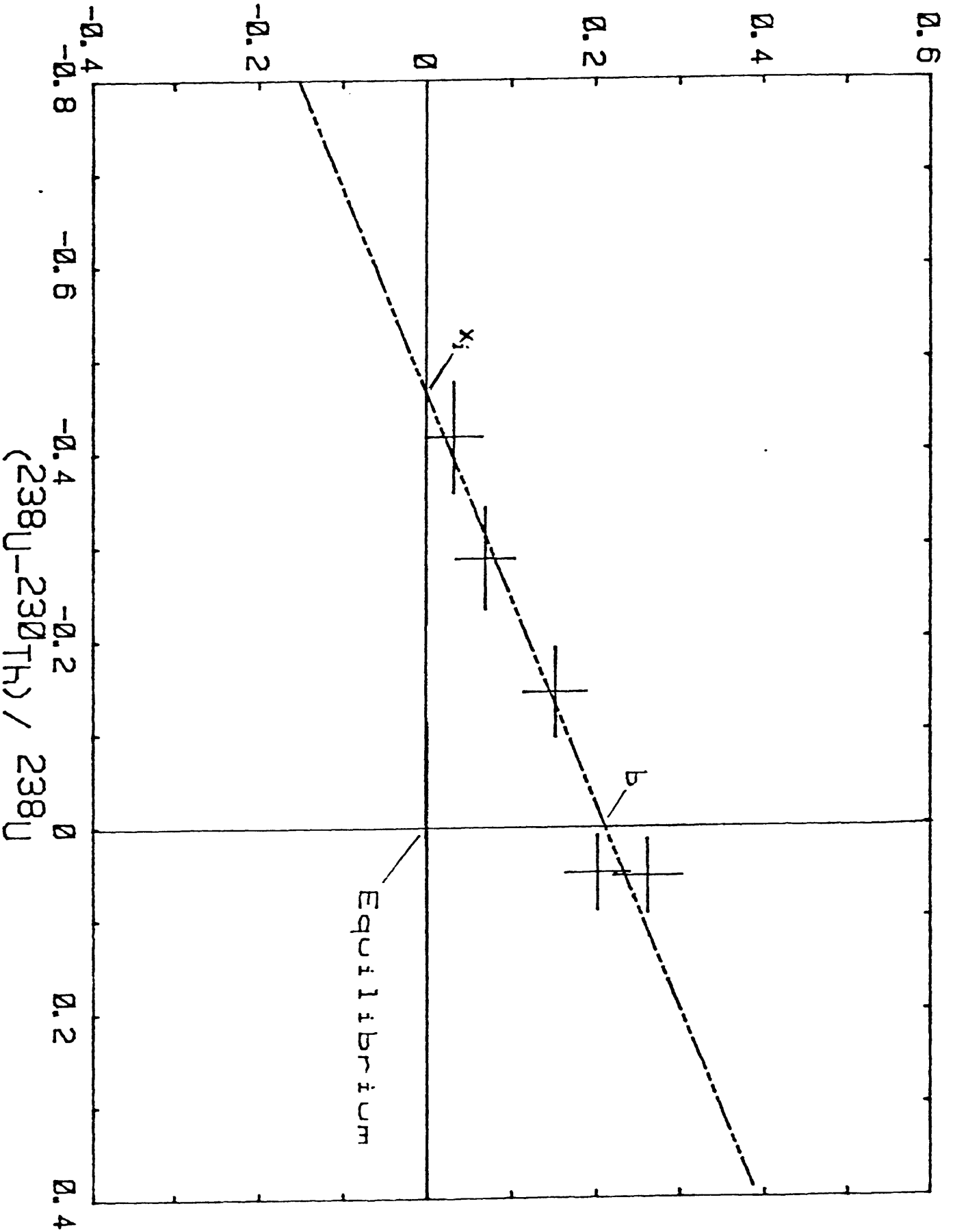


Figure 2. Uranium trend plot of CCA section of alluvium, Shirley Mountains, Wyoming. A11 samples plotted in terms of activity ratios.

$^{230}\text{Th}/^{232}\text{Th}$

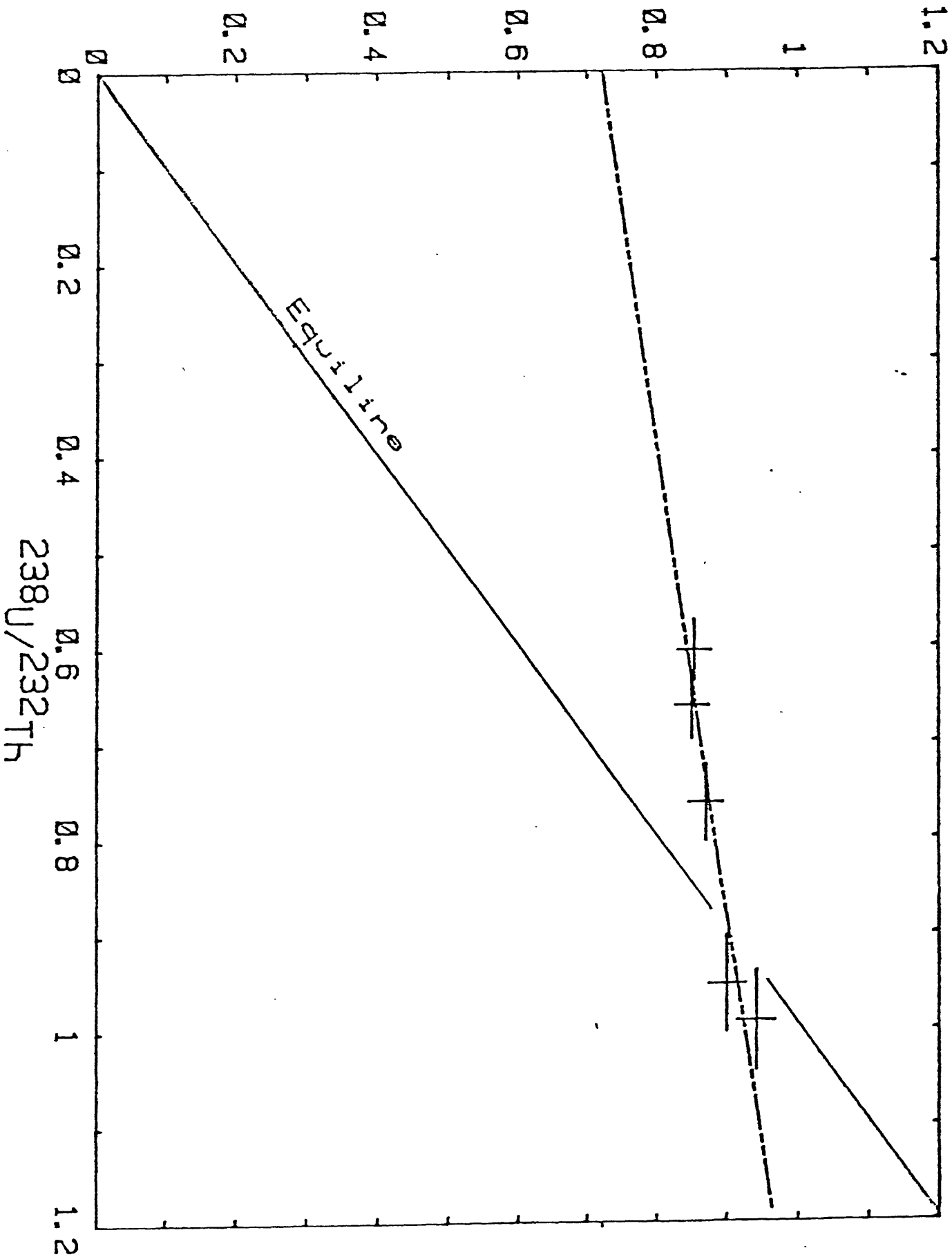


Figure 3. Thorium index plot of CCA section, Shirley Mountains, Wyoming. All samples plotted in terms of activity ratios.

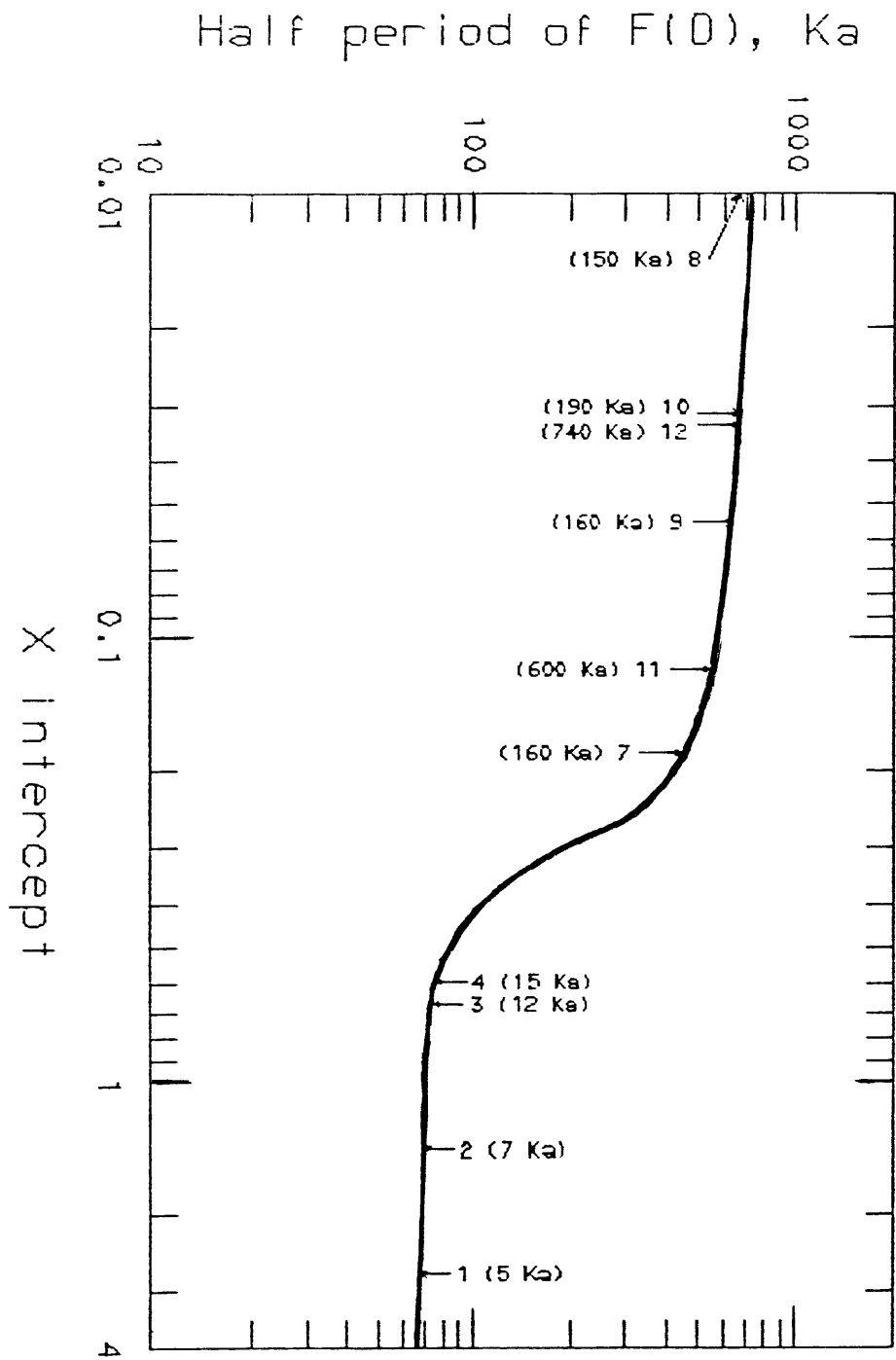


Figure 4. Time-calibration curve for determination of  $F(O)$  from X-intercept value. Indices on curve show unit number and uranium-trend age from Table 1.

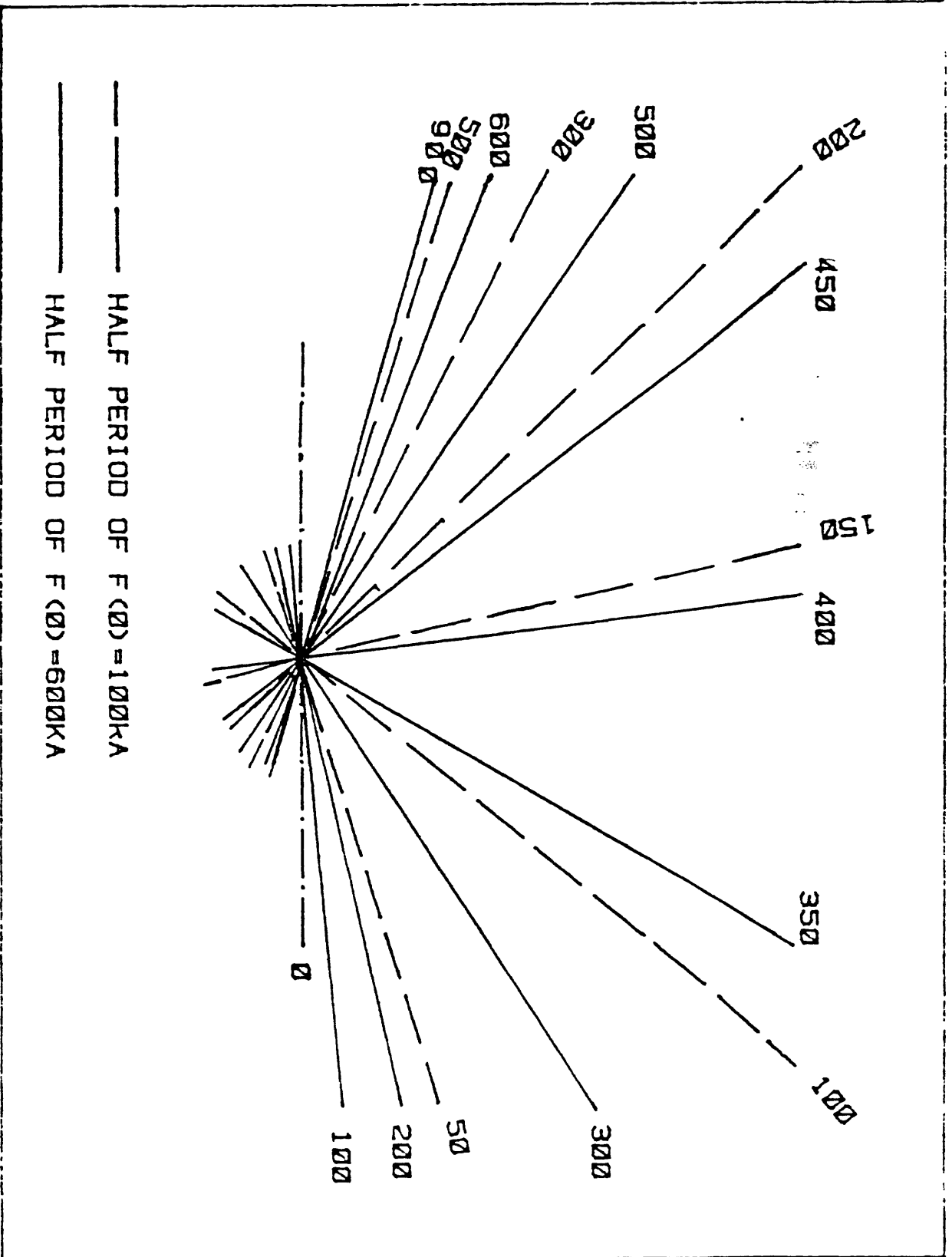
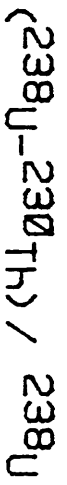


Figure 5. Variation of U-trend slope with age of deposition for 100,000 and 600,000 year half periods of  $F(0)$ .



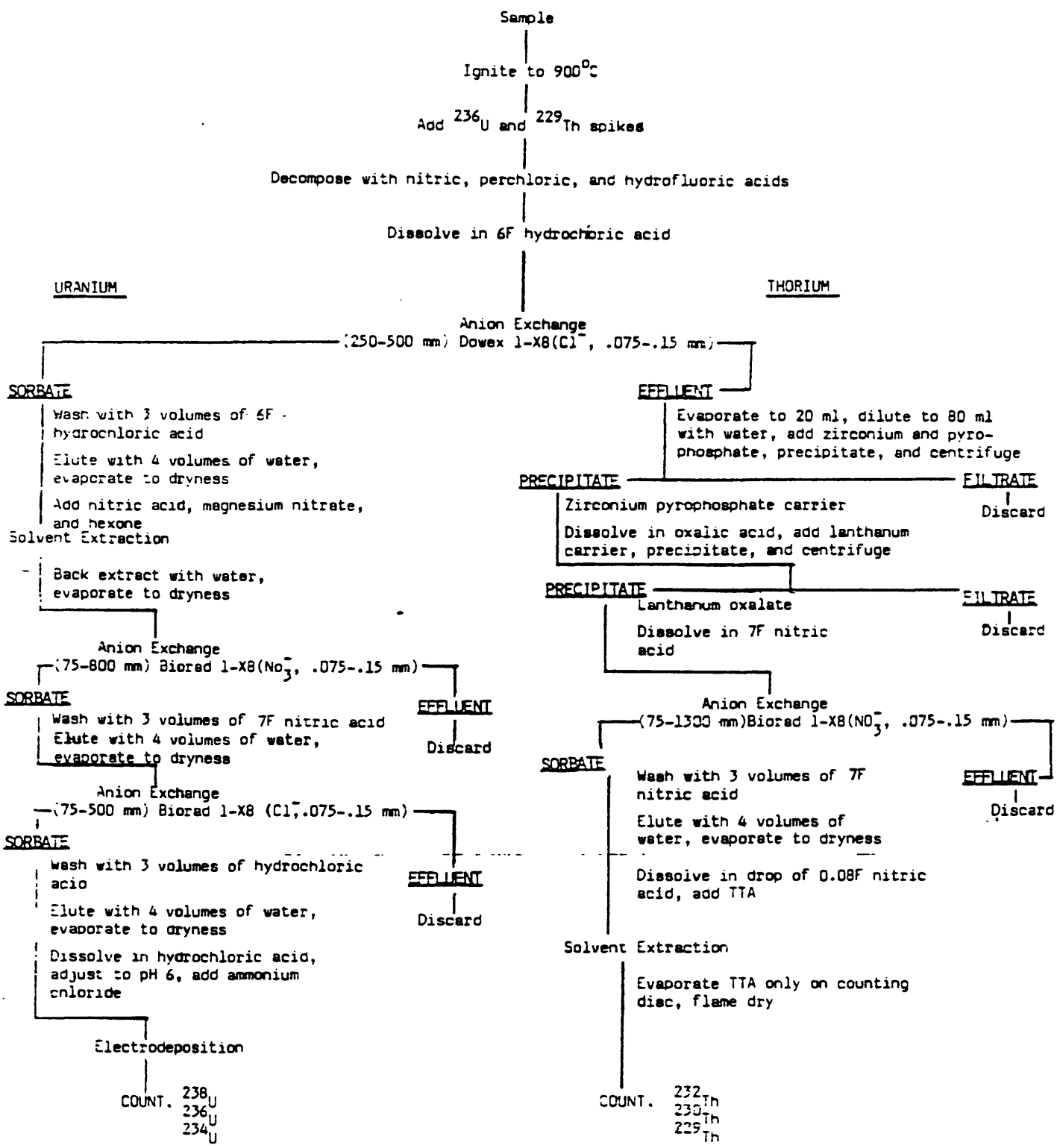


Figure 6. Schematic outline of chemical procedure.

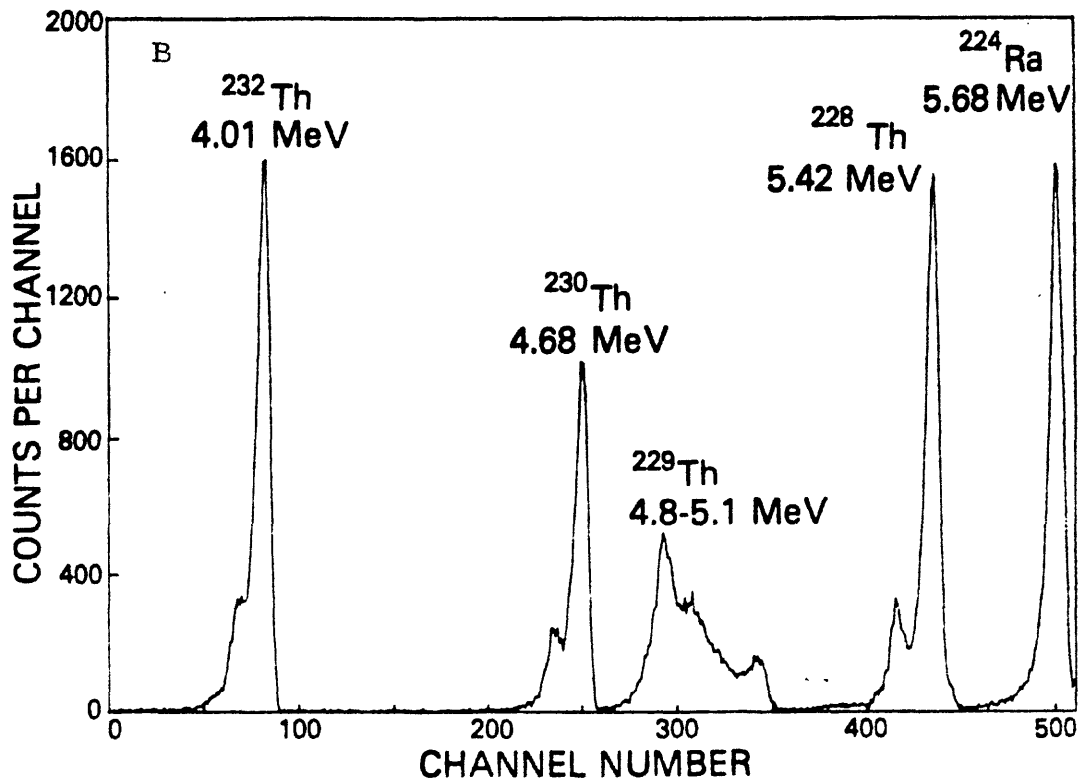
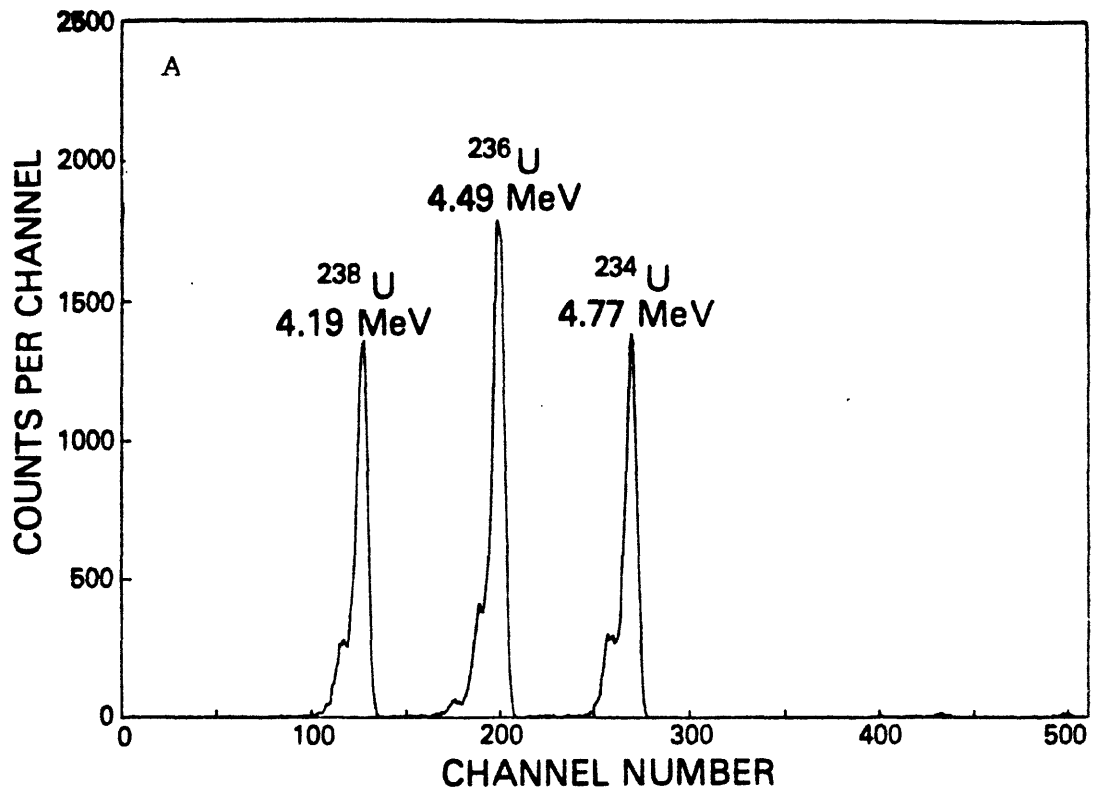


Figure 7. Alpha-particle spectra of separates. A, uranium isotopes; B, thorium isotopes.